Fatigue Strength Of Fixed Offshore Structures Under Variable Amplitude Loading Due To Wind, Wave, And Ice Action

Braun, Moritz ; Dörner, Alfons ; Willems, Tom; Seidel, Marc; Hendrikse, H.; Høyland, Knut V.; Fischer, Claas ; Ehlers, Sören

DOI
10.1115/OMAE2022-78764

Publication date
2022

Document Version
Final published version

Published in
Polar and Arctic Sciences and Technology

Proceedings of the ASME 2022 41st International Conference on Ocean, Offshore and Arctic Engineering
OMAE2022
June 5-10, 2022, Hamburg, Germany

OMAE2022-78764

FATIGUE STRENGTH OF FIXED OFFSHORE STRUCTURES UNDER VARIABLE AMPLITUDE LOADING DUE TO WIND, WAVE, AND ICE ACTION

Moritz Braun
Institute for Ship Structural Design and Analysis, Hamburg University of Technology (TUHH), Hamburg, Germany

Alfons Dörner
Institute for Ship Structural Design and Analysis, Hamburg University of Technology (TUHH), Hamburg, Germany

Tom Willems
Formerly: Siemens Gamesa Renewable Energy B.V., Den Haag, The Netherlands

Marc Seidel
Siemens Gamesa Renewable Energy GmbH & Co. KG, Hamburg, Germany

Hayo Hendrikse
Department of Hydraulic Engineering, Delft University of Technology, Delft, the Netherlands

Knut V. Høyland
Department of Civil and Environmental Engineering, the Norwegian University of Science and Technology (NTNU), Trondheim, Norway

Claas Fischer
TÜV NORD EnSys GmbH & Co. KG, Hamburg, Germany

Sören Ehlers
Institute of Maritime Energy Systems, German Aerospace Center (DLR), Geesthacht, Germany

ABSTRACT

Fixed offshore wind turbines are increasingly developed for high latitude areas where not only wind and wave loads need to be considered, but also moving sea ice. Current structural design rules do not adequately consider the effect of ice loading on fatigue life, due to missing studies on fatigue strength of welded joints under combined wind, wave, and ice action. Thus, a methodology to determine combined variable-amplitude loading (VAL) spectra was developed in a previous study. The stress state time-history at an exemplarily selected point in the support structure of an offshore wind energy monopile was translated into a VAL sequence. This sequence is used as an input for fatigue tests of butt-welded joints in the current study. The current study presents the VAL spectrum and the corresponding VAL time series, the results of the fatigue tests and compares them to typical fatigue damage sums for other stress spectra.

Keywords: Arctic technology, Ice loads, Stress analysis, Offshore Renewable Energies, Wind turbine fatigue damage and life extension, Structural integrity

NOMENCLATURE

$\Delta\sigma_n$	Nominal stress range
$\sigma_{a,i}$	Load amplitudes of the rainflow-counted spectrum
$\sigma_{a,max}$	Maximum load amplitude of the spectrum
σ_{lower}	Lower stress
σ_{upper}	Upper stress
$\Delta\sigma_R$	Reference fatigue strength at 2×10^6 cycles
D_{real}	Real fatigue damage
D_{spec}	Partial fatigue damage of the spectrum
k	Inverse slope exponent
L_s	Sequence length
n	Number of cycles of the rainflow-counted spectrum
N	Number of cycles
$\bar{N}_{exp}$	Experimental number of cycles to failure of the variable amplitude test specimens
R	Stress ratio
CAL	Constant-amplitude loading
CDF	Cumulative distribution functions
DLC	Design load case
OWT	Offshore wind turbine
VAL	Variable-amplitude loading

1. INTRODUCTION

Fixed offshore wind turbines (OWTs) continue to be developed for high latitude areas where moving sea ice is driving structural design [1]; yet, effects of ice-induced loads and the consequences for fatigue life of OWTs are still not fully

understood [2-4]. In general, it is known that ice loads on fixed offshore structures can be much higher than those from wind and wave loading [5-8]. In addition, fatigue strength typically increases at sub-zero temperatures (above the fatigue ductile-brittle transition temperature) [9-15]; however, there are currently no methods available to assess the complex interaction of low temperatures and ice loads in combination with wind and wave loads.

Fatigue design of OWTs is typically performed by means of stress-based fatigue assessment methods calibrated to constant amplitude loading (CAL) data, linear damage accumulation hypothesis, and representative load spectra or time series [12, 16-20]. For scenarios that differ from the usual loading scenarios, calibration using variable-amplitude loading (VAL) testing is required to verify applicable damage sums or similar quantities. Differences are expected due to high stresses with low occurrence probability caused by ice action, see [21]. Similar effects are well-known from overloading events, e.g., during storms [22-24].

To this day, there has never been any fatigue testing for combined wind, wave and ice load spectra. Thus, this study presents fatigue test results of an exemplary butt joint in an OWT under combined VAL due to wind, wave, and ice action. This is achieved by determination of a standardized load sequence from a numerical model that represents a case study for an OWT subjected to a number of drifting ice events during its lifetime, see [20]. To this goal, the occurrence of different load cases on an OWT in the southern Baltic Sea was simulated to obtain the structural response of an exemplary monopile support structure. This data was then analyzed to derive load spectra and time series at an exemplary welded joint of the OWT.

The current study presents the VAL spectrum and the corresponding VAL time series (Section 2), the results of the fatigue tests (Section 3) and compares them to typical fatigue damage sums for regular and similar stress spectra (Section 4).

2. COMBINED LOAD SPECTRA AND TIMES SERIES FOR WIND, WAVE, AND ICE ACTION

In the first pre-processing step, a critical load case assumption for the fatigue limit state must be defined. This has been done according to IEC61400-3-1 [25] for an exemplary monopile support structure in the southern Baltic Sea with site-specific wind and wave data, and estimated ice event conditions in Braun et al. [20]. These loads have been applied in two different modes of the turbine (idling and in operation). The defined scenarios are originally categorized in 11 design load cases (DLCs), which are regrouped in four main DLCs: operation with and without ice loading (DLC 1.2 and DLC D4), and idling with or without ice loading (DLC 6.4 and DLC D7).

2.1 Development of Combined Load Spectra from Short-Term Stress-Time Series

Due to different probabilities of load scenarios (for instance different direction of wind and waves), the structural response around the circumference of the butt joint varies significantly. Thus, the methodology proposed by Milaković et al. [2] and Braun et al. [20], and presented in Figure 1, was adopted to determine combined load spectra and time series. The stress-time series obtained from the numerical simulations are assessed (in 30° steps around the circumference) using rainflow counting. Next, the obtained range pairs are grouped into cumulative distribution functions (CDF) and superimposed. Finally, to shorten fatigue testing based on the combined load spectra, an omission level is introduced to remove low load cycles that do not contribute significantly to fatigue damage.

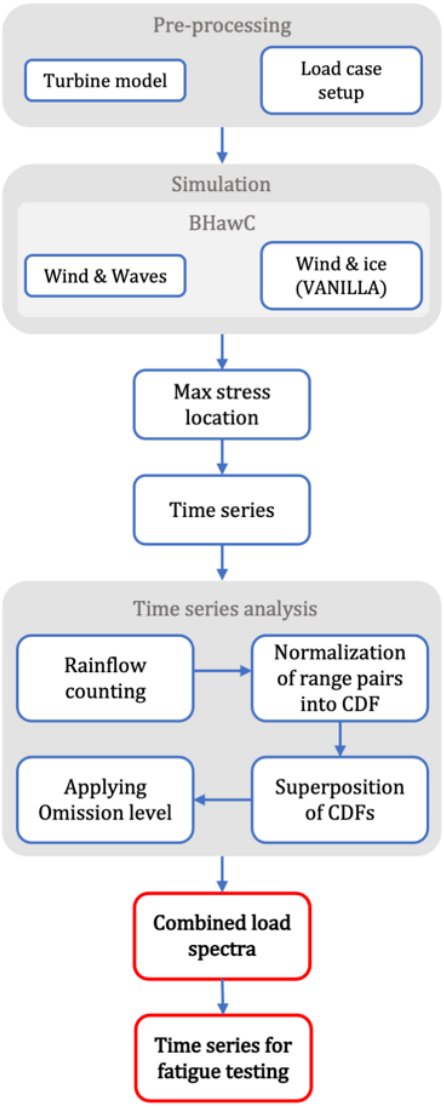

FIGURE 1: FLOWCHART OF THE DATA PROCESSING TO GENERATE COMBINED LOAD SPECTRA AND TIME SERIES OF STRUCTURAL RESPONSE [2, 20]

Once the stresses are distributed into 12 different positions around the circumference, CDFs of stresses can be calculated for each DLC and 30° sector. Next, the stress spectra obtained for each DLC are added up to determine a combined load spectra for

wind, wave and ice action for each 30° sector. This is presented in Figure 2 exemplarily for the 150° sector.

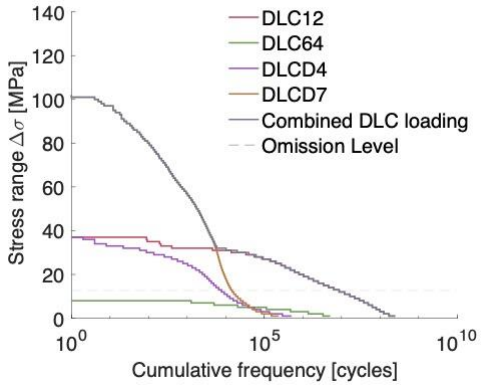

FIGURE 2: EXEMPLARY DERIVED LOAD SPECTRA FOR THE DIFFERENT DLCS AND AN ESTIMATED SERVICE LIFE OF 23.27 YEARS

2.2 Derivation of Stress-Time Series for Fatigue Testing

During rainflow counting, the transitions from upper and lower stress levels as well as mean values are stored in transition matrices (also called Markov matrices). As the probability of different stress levels and the number of occurred transitions remain after superposing the different load cases, stochastic signals can accurately be synthesized by inverting this process. For this purpose, the Markov matrices are subdivided into 64 classes ranging from the lowest to the highest stress level determined by rainflow counting. Load stress transitions were then removed by applying an omission of 10% of the maximum stress range. Applying the omission level before determining stress-time series reduces computation times significantly.

The stress-time series in terms of turning points are then created by means of Markov chain method, which creates a discrete sequence of transitions. A stochastically distributed probability of an occurring state is assigned by normalizing the matrix row by row and creating a single uniformly distributed random number in the interval [0, 1]. The following item is selected based on the previous, a new random number and so on. A comprehensive explanation is presented in Krüger et al. [26]. A sequence from the stress-time series obtained for the 150° sector is exemplarily presented in Figure 3. To highlight the magnitude of stresses related to large ice loads, the maximum stress is displayed in the middle of the sequence with 400 turning points before and after the maximum. In addition, a changing mean stress level can be seen from Figure 3. This is another important aspect of stress signal reconstruction by the Markov chain method.

3. RESULTS AND DISCUSSION

3.1 Fatigue Testing of Exemplary Butt Joints of an Offshore Wind Turbine Support Structure

The thickness of the steel plates is 17 mm at the exemplary butt joint below the nacelle of the OWT. To be able to perform tests at room and sub-zero temperatures, it was decided to scale the test specimens to 10 mm thickness. Below 25 mm plate thickness, it is usually assumed that the fatigue strength is not influenced by the so-called thickness effect [27]. This was confirmed by additional tests with 17 mm thick specimens.

FIGURE 4: A FAILED FATIGUE TEST SPECIMEN IN THE HYDRAULIC TEST RIG

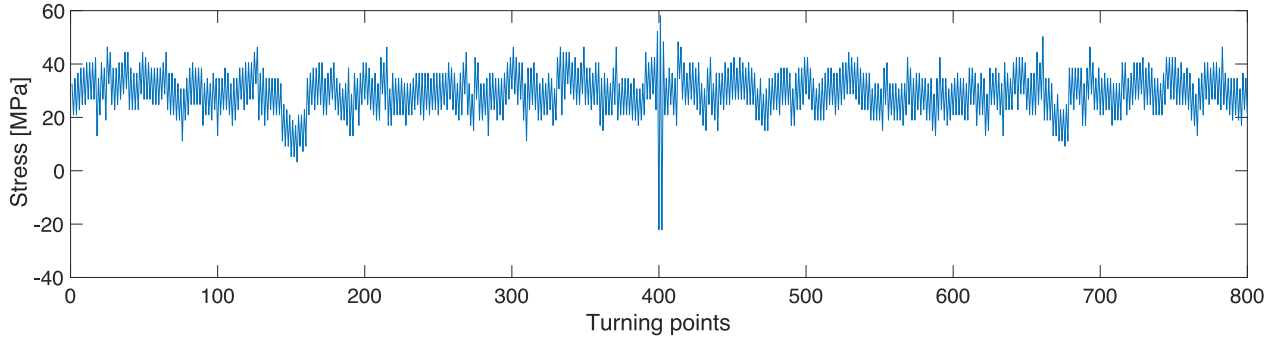

FIGURE 3: STRESS-TIME SERIES CREATED BY MEANS OF MARKOV CHAIN METHOD WITH 400 TURNING POINTS AROUND THE MAXIMUM LOAD AND AN APPLIED OMISSION LEVEL OF 10%

The CAL tests were performed in a Schenk resonance fatigue test rig and the VAL tests in a servo-hydraulic test rig, see Figure 4 for the VAL test.

In order to analyze the effect of the combine load spectrum, only tests performed at room temperature are presented in this study. Both types of tests were performed on different load levels to enable the determination of stress-life (S-N) curves by curve fitting. To this goal, the recommendations of the German Welding Society were applied to assess the test results by linear regression [28] with:

$$N = 2 \times 10^6 \left(\frac{\Delta\sigma_n}{\Delta\sigma_R}\right)^{-k} \quad (1)$$

where N is the endured number of cycles on the nominal stress range level $\Delta\sigma_n$, $\Delta\sigma_R$ is the reference fatigue strength at $2{\times}10^6$ cycles, and k the inverse slope exponent.

Due to the moderate yield strength of the material, the range of possible stress levels for the VAL tests was limited by the yield strength. In addition, the long test duration of VAL tests also limits the range of lower stress ranges. The longest tests took about two weeks. In total, 11 VAL tests were performed.

3.2 Fatigue Test Results under Constant Amplitude and Variable Loading

The CAL tests were performed at two different stress ratios R, to account for the variability of stress ratios and the possibility of relaxation of residual stresses during the service life of an actual OWT support structure. Typically, the average mean stress level is defined by the stress ratio as the quotient of lower stress (σ_{lower}) divided by upper stress (σ_{upper}). For the presented time series this would results in a stress ratio of about -0.3, due to the compressive stress peaks caused by ice loading. In fact, the majority of load cycles related to wind and wave loading cause a high mean stress level. We therefore propose a new definition of stress ratio for VAL loading, which is the quotient of the sums of lower and upper stresses under VAL:

$$R = \frac{\sum \sigma_{lower}}{\sum \sigma_{upper}} \quad (2)$$

Based on this formula, a stress ratio of about 0.55 is calculated for the stress-time series used in this study.

The results of both types of fatigue tests are presented in Figure 5. Therein, the VAL results are presented as a Gassner curve for the maximum nominal stress range ($\Delta\sigma_{nom,max}$) and the CAL results in their typical form as S-N (or Wöhler) curves. Due to the limited range of VAL stress range levels, both the CAL and VAL tests were assessed assuming a fixed slope exponent of $k = 3$.

As there is no straight-forward approach to account for misalignment effects of VAL tests, all results are presented without a correction for secondary bending stresses created by specimen misalignments (axial and angular misalignment); however, the level of misalignment was similar for all specimens.

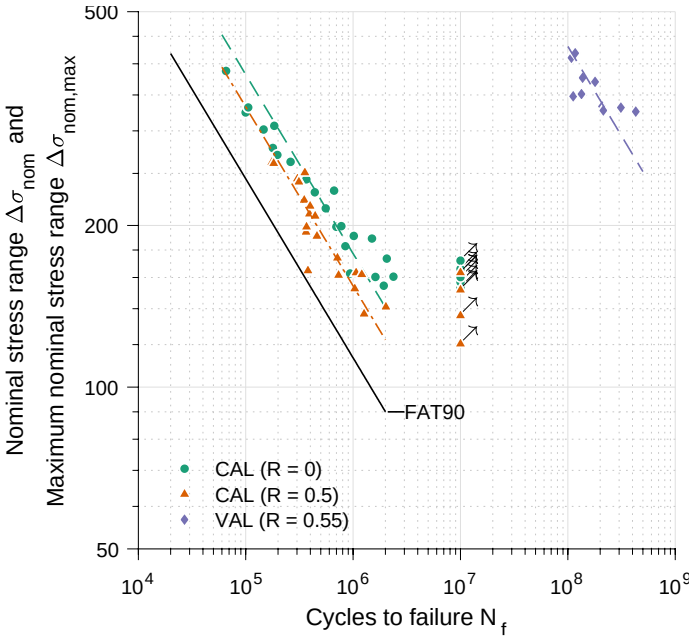

FIGURE 5: FATIGUE TEST RESULTS OF AN EXEMPLARY SCALED BUTT JOINT IN THE OWT SUPPORT STRUCTURE OF THE CASE STUDY UNDER CAL AND VAL AT ROOM TEMPERATURE; CAL RESULTS FROM [29, 30]

The VAL results are usually displayed for the full number of load cycles determined to represent one year of service, i.e., including the load cycles under the omission level. The results are presented in Figure 5 together with the CAL fatigue design S-N curve being valid for butt joints made in workshops in flat position (FAT90) and commonly used in fatigue assessment.

3.3 Determination of a Suitable Damage Sum for the Combined Load Spectra

To derive suitable damage sums for design, a linear fatigue damage accumulation calculation is performed. To this end, the Palmgren-Miner rule is applied to determine the damage of the combined load spectrum:

$$D_{spec} = \sum(n/N)_i \quad (3)$$

with n as the number of cycles of each stress block i and the corresponding endurable cycles to failure N based on the CAL S-N curves. For cycles below the fatigue limit (k_2), the well-known slope correction by Haibach [31] is applied:

$$k_2 = 2k_1 - 1 \quad (4)$$

where k_1 is the slope in the high-cycle fatigue regime (here $k_1 = 4$, see [29, 30]). To determine the representative fatigue damage of the stress spectrum, the spectrum is first subdivided into eight blocks, as presented in Figure 6.

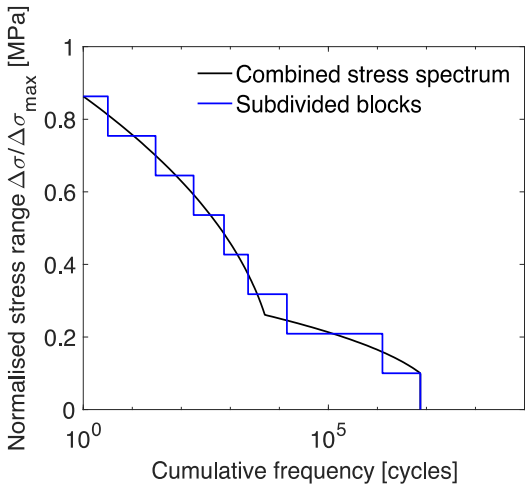

FIGURE 6: SUBDIVISION OF THE COMBINED LOAD SPECTRUM FOR THE 150° DIRECTION AND 23.27 YEARS OF SERVICE INTO EIGHT BLOCKS FOR THE FATIGUE DAMAGE CALCULATION (THE MAXIMUM STRESS RANGE IN THIS FIGURE REFERS TO HIGHEST STRESS RANGE OBSERVED FOR ANY LOADING DIRECTION OF THE CASE STRUCTURE)

After normalizing this subdivision to one year, it is possible to calculate the partial fatigue damage for each block and the fatigue damage of the spectrum (D_{spec}) by summing them up according to Eq. (3). Herein, also the stress ratio (R) for each block is accounted for by correcting the stress ranges to a stress ratio of $R = 0.5$ as recommended by the recommendations of the International Institute of Welding [27].

As the blocks represent the applied stress-time sequence of the VAL tests, it is possible to determine the real fatigue damage (D_{real}) from the partial fatigue damage of the spectrum (D_{spec}), the sequence length (L_s) and the experimental number of cycles to failure ($\bar{N}_{exp}$) each specimen endured during the VAL tests:

$$D_{real} = \frac{D_{spec}}{L_s} \cdot \bar{N}_{exp} \tag{5}$$

Using the aforementioned formulas and the S-N curve for $R = 0.5$ presented in Figure 5, the real fatigue damage (D_{real}) is determined for each of the 11 VAL tests. An estimate of a suitable damage sum for the combined stress spectrum is then obtained from the distribution of the 11 damage sums. In this case, a mean damage sum of 0.16 was determined with a standard deviation of 0.06.

4. DISCUSSION

According to Sonsino [32], about 90% of the real damage sums, are below the theoretical damage sum of 1. Recommendations for damage sums suitable for welded joints range from 0.3 [33] to 0.5 [27]; however, under fluctuating mean stresses (as in this study), real damage sums can be as low as 0.2 [34]. The low average damage sum obtained in the current study, is related to the effect of fluctuating mean stress; yet, in addition, the severity of the high stress cycles can have a significant effect on fatigue damage accumulation.

In a study on VAL tests with periodical overloads, Sonsino et al. [35] observed no change of damage sums for welded joints of various material strengths in a comparison between stress spectra with and without overloads. They attributed this effect to the residual relaxation due to yielding of the welded joints. In the current study, the maximum stress was chosen to be 70% of the base material yield strength at maximum. Any plasticity at the welded joints, is therefore limited to a small area at the weld toes, where the highest stress concentration appears. Interestingly, higher damage sums (about 0.22) are observed for the tests with the highest maximum stresses (up to 70% of the base material yield strength). For the tests with lower maximum stresses, the damage sums decrease down to a minimum of 0.08. This damage sum was observed in a test with maximum stresses corresponding to 58% of the yield strength. Thus, yielding and subsequent residual stress relaxation is unlikely. It is hence assumed that for high maximum stress levels, a certain relaxation of residual stresses occurred. For low maximum stress levels, this effect is very limited (if present at all) and the severity of the stress spectrum increases significantly.

In comparison, a damage sum below 0.1 requires a safety factor on fatigue design of more than 10. This highlights the severity of ice loads for fatigue design of structures subjected to combined wind, wave, and ice action, but also the effect of randomly distributed ice-related stress peaks. In reality, ice-related stresses are not randomly distributed between wind- and wave-related stress cycles.

In summary, the aim was to determine a conservative estimate for a damage sum applicable for combined wind, wave, and ice action. This was achieved by accounting for fluctuating mean stress level and the random mixture of stress cycles. Thus, an average damage sum of 0.16 seems reasonable. In addition, based on similarity of the overload stress spectrum investigated by Sonsino et al. [35] and the here presented stress spectrum as well, it was possible to relate the height of the damage sums to the ratio between maximum stress of the stress-time sequence and the yield strength.

The reason for the large difference between the theoretical damage sum of 1 and the determined damage sum of 0.16 is related to the underlying assumptions of Miner Palmgren-type linear damage calculation. This type of damage accumulation does not account for the sequence and mixture of loads. In addition, effects of short crack growth below the endurance limit (obtained from CAL tests) are accounted for in a simplified manner by Eq. (4). After progressive damage accumulation, load cycles below the endurance limit become harmful. As the endurance limit decreases after fatigue initiation caused by large stress cycles, also lower stress cycles can propagate fatigue cracks. A number of more advanced damage accumulation hypothesis are known to yield better results for such cases [36]; however, linear damage accumulation is basically the only method that is applied in industry.

Finally, also the introduced omission level affects the determine damage sum, as a large number of low load cycles are

neglected. This effect is, however, thought to be negligible as the chosen omission level was quite low with 10% of the normalized stress range. Recommendations range up to 50% depending on the specimen type, see [37].

Offshore structures subjected to ice loads are simultaneously exposed to sub-zero temperatures. The presented results are based on tests performed at room temperature. Thus, effects of sub-zero temperatures are not considered. In recent studies, it was determined that S-N curves are significantly affected by sub-zero temperatures [13, 14, 29]. With decreasing temperature, fatigue strength is increasing almost linearly. This effect will have a significant non-linear effect on fatigue damage under VAL due to the change of endurance limit and possible changes of slope exponent of S-N curves as well as the endurable damage sum. Hence, future studies should aim at performing such tests also under sub-zero temperatures.

5. CONCLUSIONS

This study presented fatigue test results of an exemplary butt joint in a monopile support structure subjected to constant and variable amplitude loading at room temperature. The variable amplitude loading sequence is based on a novel combined load spectra and standardized stress-time sequences for OWTs that account for wind, wave, and ice action. To this goal, the load interaction of an exemplary monopile support structure in the Baltic Sea was determined in a previous study, see [20]. In the current study, butt joints representative for monopile support structures were subjected to one stress-time sequence derived in [20]. The results were then compared to previous test results obtained under constant amplitude loading.

The presented method and results of this study are expected to serve as a foundation for future investigations on fatigue strength of OWTs under combined wind, wave, and ice action. From this study, the following conclusions are drawn:

- The constant and variable amplitude fatigue test results for the combined load spectrum (for wind, wave and ice action) led to a mean endurable fatigue damage sum of 0.16 for the investigated butt joints. Typically values for welded joint range between 0.3 and 0.5, but can be as low as 0.2 for fluctuating mean stresses. This effect is assumed to be related to the shape of the combined spectrum, the conservative mixture of stress cycles, and the underlying assumptions of the linear Palmgren-Miner damage calculation (linear damage summation, simplified modifications of the slope below the CAL endurance limit, and the neglected effect of sequence effects).
- Further studies will focus on the effect of sub-zero temperatures on fatigue strength under VAL. This will enable to accurately assess the influence of wind, wave, and ice action on fatigue life in combination with shifts of constant amplitude S-N curves due to sub-zero temperatures, as well as advanced damage accumulation theories that account for changes of slope exponents below the endurance limit.

ACKNOWLEDGEMENTS

The authors wish to acknowledge to support to the FATICE project from the MarTERA partners, the Research Council of Norway (RCN), German Federal Ministry of Economic Affairs and Energy (BMWi) through (MarTERA—FATICE (03SX465B)), the European Union through European Union's Horizon 2020 research and innovation programme under grant agreement No 728053-MarTERA and the support of the FATICE partners.

REFERENCES

[1] Shi, W., 2020, Offshore Wind Turbine-Ice Interactions, Encyclopedia of Ocean Engineering, W. Cui, S. Fu, and Z. Hu, eds., Springer Singapore, Singapore, pp. 1-13.

[2] Milaković, A.-S., Braun, M., Willems, T., Hendrikse, H., Fischer, C., and Ehlers, S., 2019, Methodology for estimating offshore wind turbine fatigue life under combined loads of wind, waves and ice at sub-zero temperatures, Proc. of International Conference on Ships and Offshore Structures ICSOS 2019 Cape Carnival, USA, November 4-8.

[3] Zhou, L., Ding, S., Song, M., Gao, J., and Shi, W., 2019, A Simulation of Non-Simultaneous Ice Crushing Force for Wind Turbine Towers with Large Slopes, Energies, 12(13).

[4] von Bock und Polach, R. U. F., Klein, M., Kubiczek, J., Kellner, L., Braun, M., and Herrnring, H., 2019, State of the Art and Knowledge Gaps on Modelling Structures in Cold Regions, Proc. of ASME 2019 38th International Conference on Ocean, Offshore and Arctic Engineering Glasgow, Scotland, June 9–14.

[5] McGovern, D. J., and Bai, W., 2014, Experimental study of wave-driven impact of sea ice floes on a circular cylinder, Cold Regions Science and Technology, 108, pp. 36-48.

[6] Hou, J., and Shao, W., Year, Structural Design for the Ice-Resistant Platform, Proc. of The Twenty-fourth International Ocean and Polar Engineering ConferenceISOPE-I-14-171.

[7] Shi, W., Tan, X., Gao, Z., and Moan, T., 2016, Numerical study of ice-induced loads and responses of a monopile-type offshore wind turbine in parked and operating conditions, Cold Regions Science and Technology, 123, pp. 121-139.

[8] Popko, W., 2020, Impact of Sea Ice Loads on Global Dynamics of Offshore Wind Turbines, Fraunhofer Verlag: Stuttgart.

[9] Walters, C. L., Alvaro, A., and Maljaars, J., 2016, The effect of low temperatures on the fatigue crack growth of S460 structural steel, International Journal of Fatigue, 82, pp. 110-118.

[10] Alvaro, A., Akselsen, O. M., Ren, X. B., and Nyhus, B., 2016, Fatigue Crack Growth of a 420 MPa Structural Steel Heat Affected Zone at Low Temperatures, Proc. of The 26th International Ocean and Polar Engineering Conference, Rhodes, Greece, June 26-July 2.

[11] Braun, M., 2021, Assessment of fatigue strength of welded steel joints at sub-zero temperatures based on the micro-structural support effect hypothesis,Doctoral Thesis, Technische Universität Hamburg.

[12] Braun, M., and Ehlers, S., 2022, Review of methods for the high-cycle fatigue strength assessment of steel structures subjected to sub-zero temperature, Marine Structures, 82.

[13] Braun, M., 2021, Statistical analysis of sub-zero temperature effects on fatigue strength of welded joints, Welding in the World.
[14] Braun, M., Scheffer, R., Fricke, W., and Ehlers, S., 2020, Fatigue strength of fillet-welded joints at subzero temperatures, Fatigue Fract Eng M, 43(2), pp. 403-416.
[15] Sallaba, F., Rolof, F., Ehlers, S., Walters, C. L., and Braun, M., 2022, Relation between the Fatigue and Fracture Ductile-Brittle Transition in S500 Welded Steel Joints, Metals, 12(3).
[16] Lotsberg, I., 2016, Fatigue Design of Marine Structures, Cambridge University Press, Cambridge.
[17] Wu, X., Hu, Y., Li, Y., Yang, J., Duan, L., Wang, T., Adcock, T., Jiang, Z., Gao, Z., Lin, Z., Borthwick, A., and Liao, S., 2019, Foundations of offshore wind turbines: A review, Renewable and Sustainable Energy Reviews, 104, pp. 379-393.
[18] Sonsino, C. M., 2011, Spectrum loading effects on structural durability of components, Structural Integrity and Life, 11(3), pp. 157-171.
[19] Heim, R., 2020, Structural Durability: Methods and Concepts, Springer International Publishing.
[20] Braun, M., Dörner, A., ter Veer, K. F., Willems, T., Seidel, M., Hendrikse, H., Høyland, K. V., Fischer, C., and Ehlers, S., 2022, Development of Combined Load Spectra for Offshore Structures Subjected to Wind, Wave, and Ice Loading, Energies, 15(2).
[21] Høyland, K. V., Nord, T., Turner, J., Hornnes, V., Gedikli, E. D., Bjerkås, M., Hendrikse, H., Hammer, T., Ziemer, G., Stange, T., Ehlers, S., Braun, M., Willems, T., and Fischer, C., 2021, Fatigue damage from dynamic ice action – The FATICE project, Proc. of 26th International Conference on Port and Ocean Engineering under Arctic Conditions, Moscow, Russia, June 14-18.
[22] Li, S., Cui, W., and Paik, J. K., 2015, An improved procedure for generating standardised load-time histories for marine structures, Proceedings of the Institution of Mechanical Engineers, Part M: Journal of Engineering for the Maritime Environment, 230(2), pp. 281-296.
[23] Hesseler, J., Baumgartner, J., and Bleicher, C., 2021, Consideration of the transient material behavior under variable amplitude loading in the fatigue assessment of nodular cast iron using the strain-life approach, Fatigue Fract Eng M, 44(10), pp. 2845-2857.
[24] Ziegler, L., Schafhirt, S., Scheu, M., and Muskulus, M., 2016, Effect of Load Sequence and Weather Seasonality on Fatigue Crack Growth for Monopile-based Offshore Wind Turbines, Energy Procedia, 94, pp. 115-123.
[25] IEC 61400-3-1:2019, Wind energy generation systems – Part 3-1: Design requirements for fixed offshore wind turbines, 2019, International Electrotechnical Commission, Genf, Switzerland.
[26] Krüger, W., Scheutzow, M., Beste, A., and Petersen, J., 1985, Markov-und Rainflow-Rekonstruktionen stochastischer Beanspruchungszeitfunktionen, Düsseldorf.
[27] Hobbacher, A. F., 2016, Recommendations for Fatigue Design of Welded Joints and Components, Springer International Publishing Switzerland.
[28] Merkblatt DVS 2403 Empfehlungen für die Durchführung, Auswertung und Dokumentation von Schwingfestigkeitsversuchen an Schweißverbindungen metallischer Werkstoffe, 2019, DVS, Düsseldorf.
[29] Braun, M., Milaković, A.-S., Ehlers, S., Kahl, A., Willems, T., Seidel, M., and Fischer, C., 2020, Sub-Zero Temperature Fatigue Strength of Butt-Welded Normal and High-Strength Steel Joints for Ships and Offshore Structures in Arctic Regions, Proc. of ASME 2020 39th International Conference on Ocean, Offshore and Arctic Engineering, Fort Lauderdale, FL, USA, June 28-July 3.
[30] Braun, M., Kahl, A., Willems, T., Seidel, M., Fischer, C., and Ehlers, S., 2021, Guidance for Material Selection Based on Static and Dynamic Mechanical Properties at Sub-Zero Temperatures, Journal of Offshore Mechanics and Arctic Engineering, 143(4), pp. 1-45.
[31] Haibach, E., 1970, Modifizierte lineare Schadensakkumulations-hypothese zur Berücksichtigung des Dauerfestigkeitsabfalls mit fortschreitender Schädigung, Laboratorium für Betriebsfestigkeit, Darmstadt, Germany.
[32] Sonsino, C. M., 2007, Fatigue testing under variable amplitude loading, International Journal of Fatigue, 29(6), pp. 1080-1089.
[33] Radaj, D., and Vormwald, M., 2007, Ermüdungsfestigkeit: Grundlagen für Ingenieure, Springer Berlin Heidelberg.
[34] Sonsino, C. M., 2005, Principles of Variable Amplitude Fatigue Design and Testing, P. C. McKeighan, and N. Ranganathan, eds., ASTM International, West Conshohocken, PA, pp. 3-23.
[35] Sonsino, C. M., Kaufmann, H., Wagener, R., Fischer, C., and Eufinger, J., 2011, Interpretation of Overload Effects under Spectrum Loading of Welded High-Strength Steel Joints, Welding in the World, 55(11-12), pp. 66-78.
[36] Zenner, H., and Liu, J., 1992, Vorschlag zur Verbesserung der Lebensdauerabschätzung nach dem Nennspannungskonzept, Konstruktion (1981), 44(1), pp. 9-17.
[37] Heuler, P., and Seeger, T., 1986, A criterion for omission of variable amplitude loading histories, International Journal of Fatigue, 8(4), pp. 225-230.